

Computational simulations of hydrogen circular migration in protonated acetylene induced by circularly polarized light

Xuetao Shi, Wen Li, and H. Bernhard Schlegel^{a)}

Department of Chemistry, Wayne State University, Detroit, Michigan 48202, USA

(Received 27 April 2016; accepted 10 August 2016; published online 30 August 2016)

The hydrogens in protonated acetylene are very mobile and can easily migrate around the C₂ core by moving between classical and non-classical structures of the cation. The lowest energy structure is the T-shaped, non-classical cation with a hydrogen bridging the two carbons. Conversion to the classical H₂CCH⁺ ion requires only 4 kcal/mol. The effect of circularly polarized light on the migration of hydrogens in oriented C₂H₃⁺ has been simulated by Born-Oppenheimer molecular dynamics. Classical trajectory calculations were carried out with the M062X/6-311+G(3df,2pd) level of theory using linearly and circularly polarized 32 cycle 7 μm cosine squared pulses with peak intensity of 5.6 × 10¹³ W/cm² and 3.15 × 10¹³ W/cm², respectively. These linearly and circularly polarized pulses transfer similar amounts of energy and total angular momentum to C₂H₃⁺. The average angular momentum vectors of the three hydrogens show opposite directions of rotation for right and left circularly polarized light, but no directional preference for linearly polarized light. This difference results in an appreciable amount of angular displacement of the three hydrogens relative to the C₂ core for circularly polarized light, but only an insignificant amount for linearly polarized light. Over the course of the simulation with circularly polarized light, this corresponds to a propeller-like motion of the three hydrogens around the C₂ core of protonated acetylene. *Published by AIP Publishing.* [<http://dx.doi.org/10.1063/1.4961644>]

INTRODUCTION

Complex chemical transformations require extensive rearrangement of nuclear configurations within the molecules, which are often achieved only by stochastic vibrational motions when thermally or electronically activated. Specific rearrangements can potentially be achieved by exciting vibrational motions coupled closely to reaction coordinates. However, such efforts do not always lead to the desired nuclear rearrangement because energy deposited in specific vibrational modes is often dissipated within 1–2 ps by intramolecular vibrational redistribution (IVR).^{1,2} However, if the energy can be deposited fast enough into the appropriate modes, the preferred reaction can occur before IVR becomes significant. Recently, in a computational simulation, we demonstrated that intense, ultrashort mid-infrared laser pulses can overcome IVR to achieve targeted nuclear rearrangement.^{3–5} In particular, for oriented ClCHO⁺ we showed that angular momentum could be deposited by circularly polarized intense mid-IR pulses.⁵ Here, we show that ultrafast mid-IR excitation can promote large amplitude nuclear motions, specifically, a propeller-like three-hydrogen migration around the C₂ core in protonated acetylene. Importantly, the sense of the “propeller” rotation can be directed by changing the helicity of the circularly polarized mid-IR pulses (left or right).

Large amplitude motions of hydrogens have been studied in a number of small molecules such as acetylene, allene, and

methanol.^{6–14} These 1,2 and 1,3 hydrogen migrations can be driven by short, intense 800 nm laser pulses. Isomerization occurs on the ground or excited states of the cations and is verified by detecting the appropriate fragment ions in coincidence. In allene, H₂CCCH₂, migration is also confirmed by the detection of H₃⁺.^{6,10,15} Another example of large amplitude hydrogen motion is the roaming reaction channel for the dissociation of CH₂O to CO + H₂.^{16–19} For reaction energies just below the C–H bond dissociation energy, a hydrogen atom can “roam” around the HCO fragment before abstracting the other hydrogen to form H₂. In each of these cases, there are large barriers for hydrogen migration on the ground state surface, and the molecule must be ionized, or strong bonds must be broken before large amplitude motion of the hydrogen can occur. By contrast, the hydrogens in protonated acetylene are very mobile and can circulate around the C₂ core with barriers of only a few kcal/mol. Laser fields in the mid-IR region couple strongly to vibrational motion and should stimulate large amplitude hydrogen motion on the ground state potential energy surface at energies well below ionization or bond dissociation.

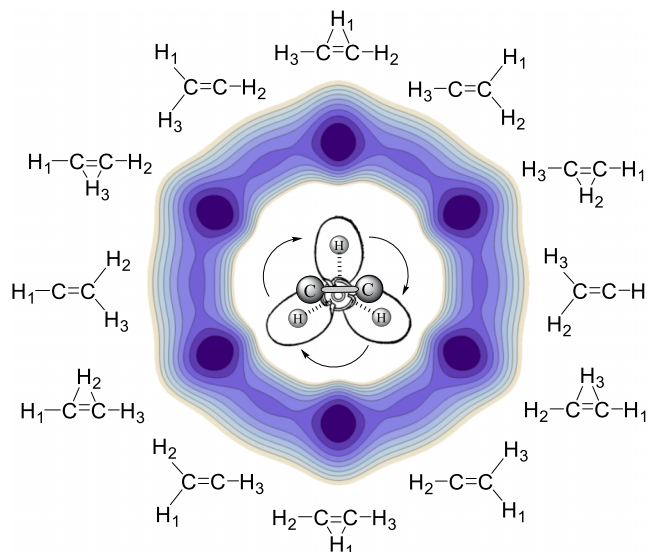
There is a long history of calculations on protonated acetylene showing that the non-classical T shaped structure, with a hydrogen bridging the two carbons, is more stable than the classical Y shaped geometry, with two hydrogens on one carbon and one hydrogen on the other carbon. Early electronic structure calculations include papers by Schaefer and co-workers,²⁰ Lindh *et al.*,^{21,22} and Curtiss and Pople.²³ Subsequent experimental work confirmed that the non-classical form is the most stable structure.^{24–27} Accurate quantum chemical calculations of the potential energy surface place the classical

^{a)} Author to whom correspondence should be addressed. Electronic mail: hbs@chem.wayne.edu.

Y shaped structure 3.7–4.0 kcal/mol above the non-classical T shaped structure.^{28,29} Recent high level calculations of the rovibrational spectrum match the experimental rotational constants to better than 0.1% and the antisymmetric HCCH stretch to within 3.0 cm^{-1} .³⁰ Large amplitude pseudorotational motion of the hydrogens has been seen under thermal conditions using Car-Parrinello simulations with both classical and path-integral dynamics.^{26,31,32} In the present study we use Born-Oppenheimer *ab initio* classical trajectory calculations to simulate the dynamics of protonated acetylene resulting from the interaction with very short, intense mid-IR pulses of linearly and circularly polarized light.

METHOD

Calculations were carried out with the development version of the Gaussian series of programs³³ using the M062X³⁴ density functional with the 6-311+G(3df,2pd)^{35,36} basis set. The choice of the functional was based on an extensive survey of ~200 functionals by comparing the energy difference between the classical (Y-shaped) and non-classical (T-shaped) structures of protonated acetylene to CCSD(T) and BD(T) calculations²⁸ (see Table S5 in the [supplementary material](#) for the functionals and energy comparisons). Classical trajectory calculations were carried out on the ground state Born-Oppenheimer surface for aligned protonated acetylene in the time varying electric field of a laser pulse. After testing various combinations of wavelengths, pulse lengths, and field strengths, the laser field was chosen to be a 32 cycle $7\text{ }\mu\text{m}$ cosine squared pulse (747 fs full width). For circularly polarized light, the propagation direction was in the z-direction perpendicular to the plane of the molecule (xy plane) with the electric field rotating in the plane of the molecule with a maximum field strength of 0.03 a.u. For linearly polarized light, the polarization direction was in the plane of the molecule, and the direction was varied from $\theta = 0^\circ\text{--}360^\circ$ in steps of 30° with a maximum field strength of 0.04 a.u. The molecular dynamics in the laser field were simulated by classical trajectory calculations which intrinsically include effects such as vibrational anharmonicity and IVR.^{37,38} Trajectories were calculated with the M062X/6-311+G(3df,2pd) level of theory using the PCvclV integrator³⁹ with a step size of 0.25 fs and Hessian updating^{40,41} for 20 steps before recalculation. Zero-point vibrational energy was added to the initial structures using orthant sampling of the momentum.⁴² Although it may not be experimentally feasible to align the molecule, the molecular dynamics calculations were carried out with protonated acetylene in the xy plane in order to maximize the effect of the circularly polarized light and to facilitate the analysis of the components of the angular motion of the hydrogens. No rotational energy was added to the initial structures so that the molecule would tend to stay in the xy plane. Trajectories were classified as either dissociating or non-dissociating based on bond lengths. Migration of hydrogen atoms was quantified by integrating the signed step-wise angular displacement of the H-(CoM)-C1 angle, projected onto xy-plane which is perpendicular to laser field propagation direction, where H is the hydrogen atom of interest, C1 is the first carbon atom, and CoM is the center of



SCHEME 1. Geometries and a representation of potential energy surface for the interchange between the T-shaped and Y-shaped structures of protonated acetylene resulting in a propeller-like motion of the hydrogens around the C_2 core.

mass of the whole molecule. To help in the analysis, the kinetic energy of the hydrogens was separated into a hydrogen circular migration component as illustrated in Scheme 1, a C–H bond stretching component and an out-of-plane component. The kinetic energy for C–H stretching was calculated from the x and y components of the velocity parallel to the vector between the hydrogen and the nearest carbon, the kinetic energy for circular migration was calculated from the x and y components of the velocity perpendicular to this vector, and the out-of-plane kinetic energy was calculated from the z component of the velocity.

RESULTS AND DISCUSSION

As illustrated in Scheme 1, the circular migration of the hydrogens in C_2H_3^+ can proceed by a sequential, stepwise interchange between the T-shaped “non-classical” structures and the Y-shaped “classical” structure. High level

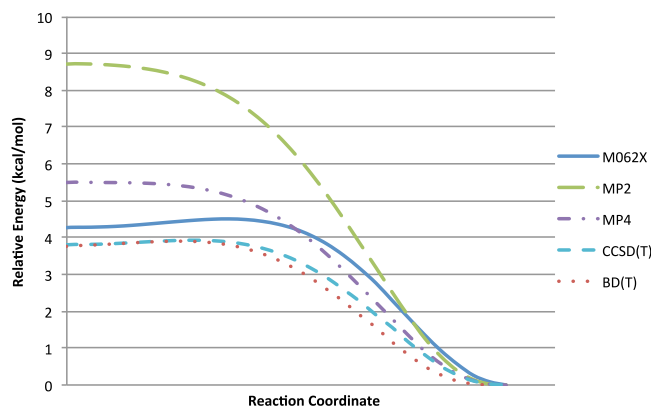
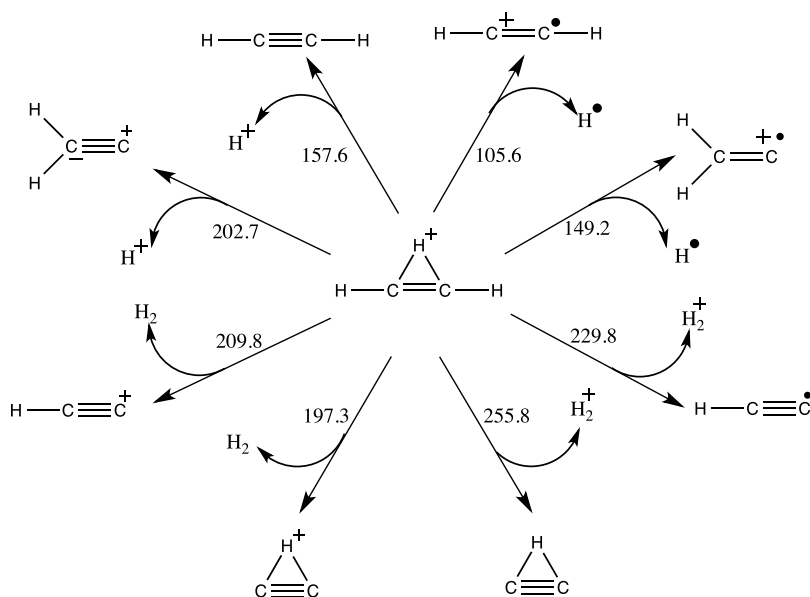


FIG. 1. Potential energy curve for protonated acetylene computed at the M062X, MP2, MP4, CCSD(T), and BD(T) levels of theory with the 6-311+G(3df,2pd) basis set.



SCHEME 2. Lowest energy dissociation channels for $C_2H_3^+$ (reaction free energies in kcal/mol at the M062X/6-311+G(3df,2pd) level of theory).

quantum calculations show that the non-classical structure is favored by 3.7–4.0 kcal/mol.^{28,29} However, these levels of theory are too costly for extensive molecular dynamics calculations. A survey of ~ 200 functionals found that the M062X/6-311+G(3df,2pd) potential energy curve is in very good agreement with accurate calculations carried out at the CCSD(T) and BD(T) levels of theory²⁸ (see Figure 1). The various channels for the dissociation of protonated acetylene are shown in Scheme 2. Since the lowest dissociation energy is ca. 100 kcal/mol, circular migration of the hydrogens can occur much more readily than dissociation.

In previous studies,^{3–5,43–45} we found that ultrashort, intense $7\ \mu\text{m}$ laser pulses were very effective at depositing vibration energy in a molecule. These studies also showed that for a given maximum field strength, circularly polarized mid-IR laser pulses deposit ca. 40% more energy than a linearly polarized pulses. In order to deposit comparable amount of energy into the molecule, a peak field strength of 0.03 a.u. was used for the circularly polarized laser field and 0.04 a.u. for the linearly polarized laser field. To determine the effect of wavelength on the response of protonated acetylene to circularly polarized light, a series of simulations was carried out with wavelengths ranging from $2\ \mu\text{m}$ to $10\ \mu\text{m}$ while keeping the pulse fixed at 32 cycles (see Table I). For shorter wavelengths, the pulse is not as wide and the interaction between the laser pulse and the molecule is considerably

TABLE I. Total energy and total angular momentum absorbed as a function of wavelength for circularly polarized light.^a

Wavelength (μm)	Percent dissociated (%)	Energy (kcal/mol)	Angular momentum (\hbar)	
			Magnitude	Z component
2	0	32.2 ± 2.4	1.8 ± 0.9	0.0 ± 1.8
3	0	44.6 ± 13.8	2.7 ± 1.6	-1.3 ± 2.3
4	0	74.4 ± 39.4	8.5 ± 5.6	-5.9 ± 6.0
5	0	71.9 ± 35.9	9.7 ± 6.1	-6.9 ± 6.3
6	0	64.4 ± 30.7	8.7 ± 6.6	-6.7 ± 6.8
7	8	148.6 ± 48.9	31.5 ± 12.2	-28.4 ± 12.3
8	16	120.8 ± 58.9	28.2 ± 16.3	-25.0 ± 15.9
9	18	160.5 ± 62.2	45.0 ± 19.9	-40.3 ± 19.3
10	36	176.0 ± 52.3	58.8 ± 19.7	-50.3 ± 18.5

^aLeft circular cosine squared pulse with 32 cycles, 50 trajectories per wavelength.

weaker than at $7\ \mu\text{m}$. Longer wavelengths (and thus wider pulses) deposited increasing amounts of energy and angular momentum. However, for wavelengths of $7\ \mu\text{m}$ and longer, the energy deposited is greater than the dissociation threshold and the number of dissociating trajectories increases markedly. Thus $7\ \mu\text{m}$ seems to be the best wavelength for the present simulations.

The effects of linear and circularly polarized light are compared in Table II. For right and left circularly polarized

TABLE II. Total energy and total angular momentum absorbed for $7\ \mu\text{m}$ linear and circularly polarized light.^a

Polarization	Field strength (a.u.)	Energy (kcal/mol)	Angular momentum (\hbar)	
			Magnitude	Z component
Left circular ^b	0.03	157.0 ± 62.6	34.0 ± 21.7	-30.3 ± 14.5
Right circular ^c	0.03	158.5 ± 77.2	33.9 ± 20.9	30.6 ± 18.1
Linear (0° – 360° averaged) ^d	0.04	158.4 ± 77.7	25.0 ± 32.2	-0.6 ± 33.1

^aCosine squared shape, $7\ \mu\text{m}$ wavelength and 32 cycles, results are averages over non-dissociating trajectories \pm one standard deviation; see Table S1 for additional data.

^b400 trajectories, ca. 4% dissociated.

^c400 trajectories, ca. 3% dissociated.

^d1200 trajectories, ca. 7% dissociated.

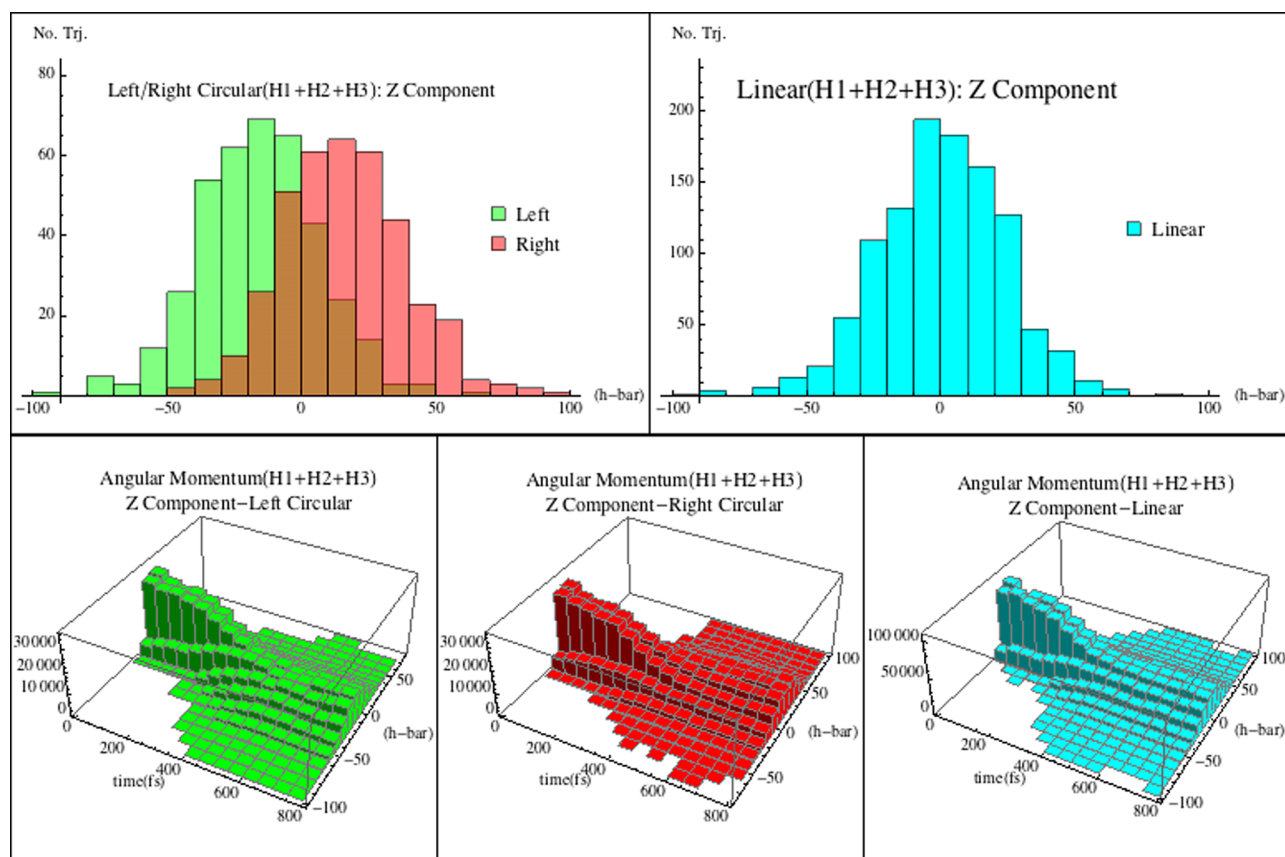


FIG. 2. Histogram of combined (H1 + H2 + H3) atomic angular momentum for left and right circularly and linearly (0° – 360° averaged) polarized at the end of simulation (top row) and over simulation time (bottom row); see Table S2 for additional data.

light, 400 trajectories were calculated for each helicity; for linearly polarized light, the polarization direction was rotated in the plane of the molecule in increments of 30° and 100 trajectories were calculated for each direction, for a total of 1200 trajectories. The average total energy absorbed is nearly the same for linearly and circularly polarized light at these field strengths. Similar to previous studies on ClCHO^+ ,⁵ the angular momentum resulting from interaction with circularly polarized light is similar in magnitude to that from linearly polarized light. For linearly polarized light the average z-component of the angular momentum is nearly zero, but for circularly polarized light the z-component strongly favors the direction corresponding to the handedness of the circular polarization. Based on the small difference between the total magnitude and z-component of the total angular momentum vectors, the majority of the total angular momentum is along the z-axis, corresponding to rotation in the molecular plane. To

determine whether the total angular momentum is indicative of a propeller-like rotation of the hydrogens requires a more detailed examination of the dynamics.

To study the rotational motion of the hydrogens with respect to C_2 core, it is helpful to break down the total angular momentum into contributions from individual atoms. As shown in Figure 2, the distribution of z-components of atomic angular momenta for the three hydrogen atoms is rather broad by the end of the simulation. The distribution for linearly polarized light is centered around zero, indicating that there is no preference in the direction of rotation. However for circularly polarized light, the distributions are displaced to either side of zero, showing that the interaction with the light results in a net rotation motion of the hydrogens in opposite directions for left and right circularly polarized light. Figure 2 also shows the evolution of the distribution of the angular momentum of the hydrogens with time. At the start of

TABLE III. Atomic kinetic energy decomposition (kcal/mol).

Polarization	Field strength (a.u.)	T_{total}	H1 + H2 + H3			C1 + C2
			T_{\perp}		T_{\parallel}	
			In-plane	Out-of-plane		
Left circular ^a	0.03	72.4 ± 31.9	15.3 ± 19.5	6.1 ± 3.9	33.8 ± 10.5	17.1 ± 7.6
Right circular	0.03	73.6 ± 40.0	16.8 ± 23.5	6.1 ± 4.1	34.3 ± 12.3	16.4 ± 7.8
Linear (0° – 360° averaged)	0.04	71.7 ± 36.4	16.1 ± 20.3	6.6 ± 5.5	32.5 ± 10.6	16.4 ± 7.8

^aSee footnotes of Table II for trajectory details; see Table S3 for additional data.

TABLE IV. Average cumulative angular displacement in the xy plane after 800 fs (in degrees).

Polarization	Field strength (a.u.)	H1	H2	H3	H1 + H2 + H3
Left circular ^a	0.03	-183.2 ± 386.0	-208.1 ± 410.2	-141.7 ± 409.5	-533.0 ± 953.5
Right circular	0.03	158.4 ± 425.1	150.3 ± 408.0	198.0 ± 429.3	506.7 ± 1052.1
Linear (0° – 360° averaged)	0.04	13.2 ± 448.3	-3.4 ± 436.2	29.9 ± 442.5	39.7 ± 1104.6

^aSee footnotes of Table I for trajectory details, displacements are averages over non-dissociating trajectories \pm one standard deviation; see Table S4 for additional data.

the simulations, the system was given zero point vibrational energy but no overall rotational energy so that it could stay aligned in the laser field. Initially, the distribution of the z-component of the angular momentum of the hydrogens is narrow and centered at zero. As time progresses, the laser field interacts with the molecule increasing the motion of the hydrogens. The distribution of the z-component of the angular momentum becomes quite broad. For linearly polarized light, the distribution remains centered around zero, but for circularly polarized light, the distribution is skewed in the positive or negative direction, depending on whether the light is right or left circularly polarized. Thus, the components of the angular momentum indicate that there is a net propeller-like motion of the hydrogens around the C₂ core.

Another way to probe the driving force behind hydrogen circular migration is to examine the kinetic energy. As shown in Table III, only about 20% of the total kinetic energy is deposited into the motion of the two carbon atoms. Because of the greater mass of carbon, the difference in kinetic energy corresponds to a significantly smaller the average velocity for the carbons than for the three hydrogens. For the hydrogens, the kinetic energy can be divided into components parallel (T_{\parallel}) and perpendicular (T_{\perp}) to the bonds between the hydrogens and the nearest carbon. The former corresponds approximately to C–H stretching motion and the latter to rotation about the C₂ core. The perpendicular component, T_{\perp} , can be further divided into in-plane rotation and motion out of the molecular plane. The in-plane T_{\perp} component of the kinetic energy corresponding to the circular migration of the hydrogen atoms, 16 kcal/mol, is only about 10% of the total energy but is more than sufficient to overcome the 4 kcal/mol energy difference

between the T-shaped and Y-shaped structures. Interestingly, the ratios of the components of the kinetic energy are nearly the same for linearly and circularly polarized light. Thus, the difference in the behavior of the molecule in linearly and circularly polarized light is not due to any difference the amount of kinetic energy deposited in various motions but is due to the difference in direction of the torque induced by the laser field.

The most direct measurement of a propeller-like hydrogen motion is simply the cumulative angular displacement of the three hydrogen atoms within the molecular plane, as measured by the change in the angle of the hydrogen with respect to the C₂ core, summed over the time steps. Since the starting geometry was chosen to be the more stable T-shaped structure with H1 as the bridging atom, there should be some difference between the initial motion of bridging hydrogen and the terminal hydrogens. Given sufficient time, all three hydrogen atoms are expected to interchange their locations, and since they are in principle indistinguishable, the sum of their individual angular displacement is a better way to monitor the rotational motion. For circularly polarized light the average displacement per hydrogen in 800 fs is about half of a full cycle, and on average motion the hydrogens move in opposite directions for left and right circularly polarized light (Table IV and Figure S1). By comparison, the average angular displacement of the hydrogens with linearly polarized light is small. For both linearly and circularly polarized light, the standard deviations are very large, indicating a wide range of magnitudes and directions for the angular displacements.

To examine the behavior of protonated acetylene at longer times, two sets of 100 trajectories were integrated for 3.2 ps

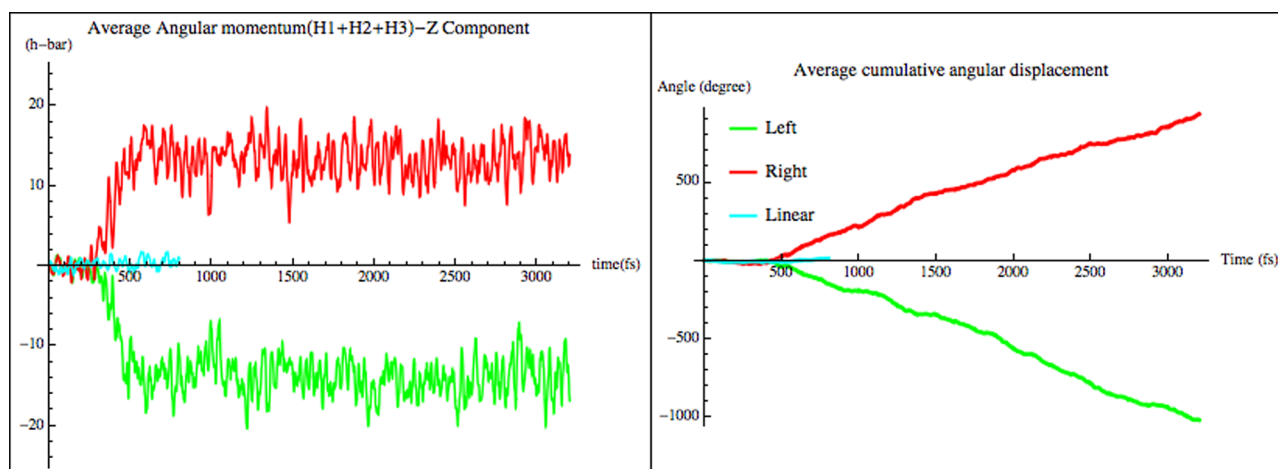


FIG. 3. Average combined hydrogen atomic angular momentum z component and cumulative average angular displacements as a function of time for non-dissociating trajectories (linear: 1200 trajectories, ca. 7% dissociated, 800 fs simulation time; left circular: 100 trajectories, ca. 15% dissociated, 3200 fs simulation time; right circular: 100 trajectories, ca. 17% dissociated, 3200 fs simulation time).

for circularly polarized light (see Figure 3). The average of the z -components of the angular momentum for the hydrogens is opposite in sign for right and left circularly polarized light. It starts to increase rapidly near the peak of the pulse, continues to rise during the second half of the laser pulse (375–750 fs), and remains nearly constant after the pulse. On average the hydrogens move in the xy plane with a standard deviation ca. 35° for the out-of-plane angle (see Figure S2) For the in-plane motion, the cumulative angular displacement of the hydrogens relative to the C_2 core starts to increase near the pulse maximum and continues to increase linearly after pulse, as expected from the z -component of the angular momentum. The standard deviation for the displacements also continues to grow nearly linearly with time after the end of the pulse. This indicates that net circulation of the hydrogens is composed of a range of rotational directions and velocities, and that this motion continues after the pulse. The fact that the z -component of the angular momentum of the hydrogens does not decrease toward zero in the 2.4 ps after the pulse (corresponding, that the angular displacement does not slow down) suggests that the circulatory motion of the hydrogens may be weakly coupled to the other vibrational modes, and that IVR is somewhat slower for this motion.

SUMMARY

In the present study we have examined the possibility of circularly polarized light inducing the propeller-like motion of hydrogen migration in $C_2H_3^+$. Circularly polarized light with a peak field strength of 0.03 a.u. is as effective as linearly polarized light with a peak field strength 0.04 a.u. in depositing kinetic energy and angular momentum for the hydrogens. For circularly polarized light, the sign of the z -component of the average angular momentum of the hydrogens depends on the handedness of the circular polarization. By comparison, the z -component of the average angular momentum is near zero for linearly polarized light. Circularly polarized light produces an appreciable amount of angular displacement of the three hydrogen atoms, corresponding to a propeller-like motion of the hydrogens around the C_2 core. By contrast, the cumulative angular displacement for linearly polarized light was very small. The total energy and kinetic energy absorbed are similar for right and left circularly polarized light, but the angular momentum vectors and cumulative angular displacement have opposite directions depending on the laser polarization handedness. The propeller-like motion of the hydrogens continues for a few ps after the laser pulse.

SUPPLEMENTARY MATERIAL

See [supplementary material](#) for additional tables and figures of energies, angular momenta, and displacements and for the density functionals used in the survey.

ACKNOWLEDGMENTS

Research was supported by the U.S. Department of Energy (DOE), Office of Science, Basic Energy Sciences

(BES), under Award No. DE-SC0012628. We thank Wayne State University's computing grid for computer time.

- ¹D. J. Nesbitt and R. W. Field, "Vibrational energy flow in highly excited molecules: Role of intramolecular vibrational redistribution," *J. Phys. Chem.* **100**, 12735 (1996).
- ²P. A. Schulz, A. S. Su, D. J. Krajnovich, H. S. Kwok, Y. R. Shen, and Y. T. Lee, "Multiphoton dissociation of polyatomic molecules," *Annu. Rev. Phys. Chem.* **30**, 379 (1979).
- ³S. K. Lee, A. G. Suits, H. B. Schlegel, and W. Li, "A reaction accelerator: Mid-infrared strong field dissociation yields mode-selective chemistry," *J. Phys. Chem. Lett.* **3**, 2541 (2012).
- ⁴S. K. Lee, H. B. Schlegel, and W. Li, "Bond-selective dissociation of polyatomic cations in mid-infrared strong fields," *J. Phys. Chem. A* **117**, 11202 (2013).
- ⁵X. Shi, B. Thapa, W. Li, and H. B. Schlegel, "Controlling chemical reactions by short, intense mid-infrared laser pulses: Comparison of linear and circularly polarized light in simulations of $C_2H_3^+$ fragmentation," *J. Phys. Chem. A* **120**, 1120 (2016).
- ⁶M. Kubel, R. Siemering, C. Burger, N. G. Kling, H. Li *et al.*, "Steering proton migration in hydrocarbons using intense few-cycle laser fields," *Phys. Rev. Lett.* **116**, 193001 (2016).
- ⁷T. Okino, A. Watanabe, H. Xu, and K. Yamanouchi, "Ultrafast hydrogen scrambling in methylacetylene and methyl-d3-acetylene ions induced by intense laser fields," *Phys. Chem. Chem. Phys.* **14**, 10640 (2012).
- ⁸H. Ibrahim, B. Wales, S. Beaulieu, B. E. Schmidt, N. Thire *et al.*, "Tabletop imaging of structural evolutions in chemical reactions demonstrated for the acetylene cation," *Nat. Commun.* **5**, 4422 (2014).
- ⁹Y. H. Jiang, A. Rudenko, O. Herrwerth, L. Foucar, M. Kurka *et al.*, "Ultrafast extreme ultraviolet induced isomerization of acetylene cations," *Phys. Rev. Lett.* **105**, 263002 (2010).
- ¹⁰H. Xu, T. Okino, and K. Yamanouchi, "Ultrafast hydrogen migration in allene in intense laser fields: Evidence of two-body Coulomb explosion," *Chem. Phys. Lett.* **469**, 255 (2009).
- ¹¹T. Osipov, C. L. Cocke, M. H. Prior, A. Landers, T. Weber, O. Jagutzki, L. Schmidt, H. Schmidt-Bocking, and R. Dörner, "Photoelectron-photoion momentum spectroscopy as a clock for chemical rearrangements: Isomerization of the di-cation of acetylene to the vinylidene configuration," *Phys. Rev. Lett.* **90**, 233002 (2003).
- ¹²H. Xu, C. Marceau, K. Nakai, T. Okino, S. L. Chin, and K. Yamanouchi, "Communication: Two stages of ultrafast hydrogen migration in methanol driven by intense laser fields," *J. Chem. Phys.* **133**, 071103 (2010).
- ¹³H. Xu, T. Okino, T. Kudou, K. Yamanouchi, S. Roither, M. Kitzler, A. Baltuska, and S. L. Chin, "Effect of laser parameters on ultrafast hydrogen migration in methanol studied by coincidence momentum imaging," *J. Phys. Chem. A* **116**, 2686 (2012).
- ¹⁴R. Itakura, P. Liu, Y. Furukawa, T. Okino, K. Yamanouchi, and H. Nakano, "Two-body Coulomb explosion and hydrogen migration in methanol induced by intense 7 and 21 fs laser pulses," *J. Chem. Phys.* **127**, 104306 (2007).
- ¹⁵K. Hoshina, Y. Furukawa, T. Okino, and K. Yamanouchi, "Efficient ejection of H_3^+ from hydrocarbon molecules induced by ultrashort intense laser fields," *J. Chem. Phys.* **129**, 104302 (2008).
- ¹⁶D. Townsend, S. A. Lahankar, S. K. Lee, S. D. Chambreau, A. G. Suits, X. Zhang, J. Rheinecker, L. B. Harding, and J. M. Bowman, "The roaming atom: Straying from the reaction path in formaldehyde decomposition," *Science* **306**, 1158 (2004).
- ¹⁷A. G. Suits, "Roaming atoms and radicals: A new mechanism in molecular dissociation," *Acc. Chem. Res.* **41**, 873 (2008).
- ¹⁸J. M. Bowman and B. C. Shepler, "Roaming radicals," *Annu. Rev. Phys. Chem.* **62**, 531 (2011).
- ¹⁹S. A. Lahankar, S. D. Chambreau, D. Townsend, F. Suits, J. Farnum, X. Zhang, J. M. Bowman, and A. G. Suits, "The roaming atom pathway in formaldehyde decomposition," *J. Chem. Phys.* **125**, 44303 (2006).
- ²⁰T. J. Lee and H. F. Schaefer, "The classical and nonclassical forms of protonated acetylene, $C_2H_3^+$. Structures, vibrational frequencies, and infrared intensities from explicitly correlated wave functions," *J. Chem. Phys.* **85**, 3437 (1986).
- ²¹R. Lindh, J. E. Rice, and T. J. Lee, "The energy separation between the classical and nonclassical isomers of protonated acetylene. An extensive study in one- and n -particle space," *J. Chem. Phys.* **94**, 8008 (1991).
- ²²R. Lindh, B. O. Roos, and W. P. Kraemer, "A CAS SCF CI study of the hydrogen migration potential in protonated acetylene, $C_2H_3^+$," *Chem. Phys. Lett.* **139**, 407–416 (1987).

- ²³L. A. Curtiss and J. A. Pople, "Theoretical study of structures and energies of acetylene, ethylene, and vinyl radical and cation," *J. Chem. Phys.* **88**, 7405 (1988).
- ²⁴M. W. Crofton, M.-F. Jagod, B. D. Rehfuss, and T. Oka, "Infrared spectroscopy of carbo-ions. V. Classical vs nonclassical structure of protonated acetylene $C_2H_3^+$," *J. Chem. Phys.* **91**, 5139–5153 (1989).
- ²⁵C. M. Gabrys, D. Uy, M.-F. Jagod, and T. Oka, "Infrared spectroscopy of carboions. 8. Hollow cathode spectroscopy of protonated acetylene, $C_2H_3^+$," *J. Phys. Chem.* **99**, 15611 (1995).
- ²⁶L. Knoll, Z. Vager, and D. Marx, "Experimental versus simulated Coulomb-explosion images of flexible molecules: Structure of protonated acetylene $C_2H_3^+$," *Phys. Rev. A* **67**, 022506 (2003).
- ²⁷Z. Vager, D. Zajfman, T. Graber, and E. P. Kanter, "Experimental evidence for anomalous nuclear delocalization in $C_2H_3^+$," *Phys. Rev. Lett.* **71**, 4319 (1993).
- ²⁸B. T. Psciuk, V. A. Benderskii, and H. B. Schlegel, "Protonated acetylene revisited," *Theor. Chem. Acc.* **118**, 75 (2007).
- ²⁹A. R. Sharma, J. Wu, B. J. Braams, S. Carter, R. Schneider, B. Shepler, and J. M. Bowman, "Potential energy surface and MULTIMODE vibrational analysis of $C_2H_3^+$," *J. Chem. Phys.* **125**, 224306 (2006).
- ³⁰R. C. Fortenberry, X. Huang, T. D. Crawford, and T. J. Lee, "Quartic force field rovibrational analysis of protonated acetylene, $C_2H_3^+$, and its isotopologues," *J. Phys. Chem. A* **118**, 7034 (2014).
- ³¹D. Marx and M. Parrinello, "The effect of quantum and thermal fluctuations on the structure of the floppy molecule $C_2H_3^+$," *Science* **271**, 179 (1996).
- ³²J. S. Tse, D. D. Klug, and K. Laasonen, "Structural dynamics of protonated methane and acetylene," *Phys. Rev. Lett.* **74**, 876 (1995).
- ³³M. J. Frisch, G. W. Trucks, H. B. Schlegel, G. E. Scuseria, M. A. Robb *et al.*, *Gaussian Development Version, H.35* (Gaussian, Inc., Wallingford, CT, USA, 2015).
- ³⁴Y. Zhao and D. G. Truhlar, "The M06 suite of density functionals for main group thermochemistry, thermochemical kinetics, noncovalent interactions, excited states, and transition elements: Two new functionals and systematic testing of four M06-class functionals and 12 other functionals," *Theor. Chem. Acc.* **120**, 215 (2007).
- ³⁵M. J. Frisch, J. A. Pople, and J. S. Binkley, "Self-consistent molecular orbital methods 25. Supplementary functions for Gaussian basis sets," *J. Chem. Phys.* **80**, 3265 (1984).
- ³⁶R. Krishnan, J. S. Binkley, R. Seeger, and J. A. Pople, "Self-consistent molecular orbital methods. XX. A basis set for correlated wave functions," *J. Chem. Phys.* **72**, 650 (1980).
- ³⁷J. M. G. Llorente and E. Pollak, "Classical dynamics methods for high energy vibrational spectroscopy," *Annu. Rev. Phys. Chem.* **43**, 91 (1992).
- ³⁸T. Baer and W. L. Hase, *Unimolecular Reaction Dynamics: Theory and Experiments* (Oxford University Press, 1996).
- ³⁹H. B. Schlegel, "Molecular dynamics in strong laser fields: A new algorithm for *ab initio* classical trajectories," *J. Chem. Theory Comput.* **9**, 3293 (2013).
- ⁴⁰V. Bakken, J. M. Millam, and H. Bernhard Schlegel, "*Ab initio* classical trajectories on the Born–Oppenheimer surface: Updating methods for Hessian-based integrators," *J. Chem. Phys.* **111**, 8773 (1999).
- ⁴¹H. Wu, M. Rahman, J. Wang, U. Louderaj, W. L. Hase, and Y. Zhuang, "Higher-accuracy schemes for approximating the Hessian from electronic structure calculations in chemical dynamics simulations," *J. Chem. Phys.* **133**, 074101 (2010).
- ⁴²D. L. Bunker, "On non-RRKM unimolecular kinetics: Molecules in general, and CH_3NC in particular," *J. Chem. Phys.* **59**, 4621 (1973).
- ⁴³S. K. Lee, W. Li, and H. Bernhard Schlegel, "HCO+ dissociation in a strong laser field: An *ab initio* classical trajectory study," *Chem. Phys. Lett.* **536**, 14 (2012).
- ⁴⁴B. Thapa and H. B. Schlegel, "Molecular dynamics of methylamine, methanol, and methyl fluoride cations in intense 7 micron laser fields," *J. Phys. Chem. A* **118**, 10067 (2014).
- ⁴⁵B. Thapa and H. B. Schlegel, "Molecular dynamics of methanol cation (CH_3OH^+) in strong fields: Comparison of 800 nm and 7 μm laser fields," *Chem. Phys. Lett.* **610-611**, 219 (2014).